Review Paper

Behavioral Analysis of Daily Rainfall Pattern in Katsina

ABSTRACT

Aims: This paper seeks to undertake a behavioral analysis of the rainfall pattern in Katsina in a view to characterizing the rainfall data and describing its dynamics so that adequate recommendations can be made for its modelling.
Study design: The analysis involves a complete statistical, trend, spectral and nonlinear analysis of the daily rainfall time series recorded in Katsina.
Place and Duration of Study: Location: Katsina City, Katsina State, Nigeria from 1990 to 2015; a period of 26 years.
Methodology: Secondary data of daily rainfall recorded in Katsina from 1990 to 2015 was collected from the Nigerian Meteorological Agency (NiMet) and then subjected to statistical, trend, spectral and nonlinear analysis techniques so as to reveal the behavioral patterns in the rainfall and also to reveal its underlying dynamics for its future modelling and prediction.
Results: The outcome of this analysis indicates that the rainfall in Katsina exhibits an annual increasing trend over the past 26 years with a high variance and right-skewed distribution requiring a maximum of 5 independent variables to model its dynamics. The largest Lyapunov exponent for the rainfall time series in Katsina was also computed and found to be -0.001157/day indicating a dissipative (stable fixed point) behavior while the correlation exponent plot failed to reach a saturation value confirming that the daily rainfall in Katsina over the last 26 years exhibits a stochastic behavior.
Conclusion: Since from the findings of this work it is confirmed that the rainfall in Katsina exhibits stochastic behavior, it is recommended that more drainages and dams be built to provide steady supply of water for agricultural and domestic purposes as well as curtail the menace of flooding and drought which may occur as a result of global warming and climate change.

Keywords: Nonlinear dynamics, trend analysis, phase space reconstruction, phase portrait, correlation dimension, Lyapunov exponent.

1. INTRODUCTION

Nowadays meteorological and hydrological studies, lays huge emphasis on the modelling of time series so as to ease the designing, planning and forecasting of these natural resources. Time series represents a dynamic measure of a physical process over a given period of time and may be discrete or continuous [1]. The discovery of Chaos by Edward Lorenz in 1961 [2], has brought about a great revolution on the mode of understanding and expressing most of these phenomena in nature. Chaos theory, the basis and foundation of nonlinear dynamics, is a tool that can be used for characterizing and modelling complex phenomena in nature such as rainfall data which has a higher variation coefficient [3]. Weather is a continuous, data-intensive, multidimensional, dynamic and chaotic process and these properties make weather prediction a big challenge as the chaotic nature of the atmosphere implies the need for massive computational power required to solve the equations that describe the atmospheric conditions [4]. Climate indeed varies nonlinearly too, but this has not prevented scientists from making good predictions using advance regression techniques. Science and technology has been applied to predict the state of the atmosphere in future time for a given location and this is very important

as it affects life on earth. Today, computational weather forecasts are made by collecting quantitative data about the current state of the atmosphere and using scientific understanding of atmospheric processes to numerically project how the atmosphere will evolve, but due to an incomplete understanding of the chaotic atmospheric processes, forecasts become less accurate as the range of forecast increases [5].
This paper is focused on undertaking a detailed behavioral analysis of the rainfall in Katsina over the last twenty-six years so as to unveil its dynamics thereby characterizing the data for modelling and forecasting to boost the planning of agricultural activities in the nearest future.

2. MATERIAL AND METHODS

The behavioral analysis of daily rainfall in Katsina state will be undertaken in this research by applying the following techniques: statistical analysis of the data, trend and spectral analysis, and nonlinear analysis.

2.1 Statistical Analysis

Statistical analysis involves the computation of the arithmetic mean, variance and standard deviation, coefficient of variation, signal-to-noise ratio, range, kurtosis and skewness. Skewness is a measure of the asymmetry of the data around the sample mean. If skewness is negative, the data are spread out more to the left of the mean than to the right. If skewness is positive, the data are spread out more to the right. The skewness of the normal distribution (or any perfectly symmetric distribution) is zero. The skewness, S of a distribution with mean μ and standard deviation σ is given as [6]:

$$S = \frac{E(x-\mu)^3}{\sigma^3} \tag{1}$$

The parameter $E(t)$ represents the expectation value of the quantity t. Kurtosis on the other hand is a measure of how outlier-prone (scattered and detached) a distribution is. The kurtosis of the normal distribution is 3 while distributions that are more outlier-prone than the normal distribution have kurtosis greater than 3; with distributions that are less outlier-prone have kurtosis less than 3. The kurtosis, K of a distribution with mean μ and standard deviation σ is given as [6]:

$$K = \frac{E(x-\mu)^4}{\sigma^4} \tag{2}$$

MATLAB statistics toolbox (R2014a) is used to achieve these computations.

2.2 Trend Analysis

In order to check the overall effect of greenhouse effect and global warming on the rainfall pattern in Katsina, trend analysis was carried out using the following statistical tools:

i. the correlation coefficient of the rainfall data with time was computed to determine the strength of the linear relationship the daily rainfall data with time,
ii. the monotonic increasing or decreasing trend was tested using the non-parametric Mann-Kendall test, and
iii. the slope of a linear trend is estimated with the nonparametric Sen's slope estimator.

2.2.1 Correlation coefficient

The Pearson product moment correlation coefficient R, measures the strength and the pattern of a linear relationship between two variables. It is mathematical given by [7]:

$$R = \frac{n\sum xy-(\sum x)(\sum y)}{\sqrt{n(\sum x^2)-(\sum x)^2}\sqrt{n(\sum y^2)-(\sum y)^2}} \tag{3}$$

R value ranges from –1 to +1, with +1 or –1 indicating a perfect correlation and a correlation coefficient close to or equal to zero indicating no relationship between the variables. A correlation greater than 0.8 is generally described as strong, whereas a correlation less than 0.5 is generally described as weak. While a positive correlation coefficient indicates an increasing trend, a negative correlation coefficient indicates a decreasing trend.

2.2.2 Mann-Kendall analysis

The nonparametric Mann-Kendall test is usually used to detect trends that are monotonic but not necessarily linear. The Mann-Kendall test statistic S is computed using the formula [8]:

$$S = \sum_{k=1}^{n-1} \sum_{j=k+1}^{n} sign(x_j - x_k), \tag{4}$$

Where x_j and x_k are the daily rainfall values and time in days j and k, with $j > k$, respectively. The sign ( ) function is defined as [9]:

$$sign(x_j - x_k) = \begin{cases} 1 & if\ x_j - x_k > 0 \\ 0 & if\ x_j - x_k = 0 \\ -1 & if\ x_j - x_k < 0 \end{cases} \tag{5}$$

A very high positive value of S (>120) is an indicator of an increasing trend, while a very low negative value indicates a decreasing trend [10]. The Man-Kendall parameter *S* and its variance *VAR(S)* are used to compute the test statistic *Z* as follows [8]:

$$Z = \begin{cases} \frac{S-1}{\sqrt{VAR(S)}} & if\ S > 0 \\ 0 & if\ S = 0 \\ \frac{S+1}{\sqrt{VAR(S)}} & if\ S < 0 \end{cases} \tag{6}$$

The Z statistic follows a normal distribution trend, is tested at 95% (α=0.05) level of significance ($Z_{\frac{\alpha}{2}} = 1.96$) and its value describes the trend as [11]:

i. decreasing if Z is negative and the absolute value is greater than the level of significance,
ii. increasing if Z is positive and greater than the level of significance, and
iii. no trend if the absolute value of Z is less than the level of significance.

2.2.3 Sen's slope estimator

The Sen's test estimates the true slope of an existing trend (i.e. change per day). The Sen's method is used in cases where the trend can expressed as linear:

$$y(t) = Qt + B \tag{7}$$

Where Q is the slope, B is a constant and *t* is time.

$$Sen's\ estimator,\ Q = \underset{j>k}{median}\left(\frac{x_j - x_k}{j-k}\right) \tag{8}$$

For *n* values x_j in the time series there will be as many as $N = \frac{n(n-1)}{2}$ slope estimates Q_i of which the median value gives the Sen's estimator, Q. In order to get an estimate of the intercept B in equation (7), the *n* values of differences $x_i - Qt_i$ are calculated and the median of these values gives an estimate of B [12].

2.3 Spectral Analysis

Spectral analysis is another simple way of characterizing attractors and is often used to qualitatively distinguish quasi-periodic or chaotic behavior from periodic structure and also to identify different periods embedded in a chaotic signal. Chaotic signals are characterized by the presence of wide broadband noise in their power spectrum, with a continuum of frequencies in their oscillations [13]. The power spectrum of a signal shows how a signal's power is distributed throughout the frequency domain [14]. To convert the rainfall time domain series to frequency domain, the fast Fourier transform (fft) was applied. The power per Hertz is obtained from the square of the absolute value of the fast Fourier transform [15]:

$$Power/Hz = abs\{fft[x(t)]\}^2 \tag{9}$$

The periodicity of the rainfall in Katsina was estimated from the power spectrum as the reciprocal of the dominant frequency (peak or fundamental frequency) of the power spectrum plot [16].

2.4 Nonlinear Analysis

The tools of nonlinear analysis used to characterize the daily rainfall data in this paper include: time series plot, phase portrait and Poincaré map, correlation dimension, Lyapunov exponents and Kolmogorov-Sinai entropy.

2.4.1 Time series plot

Time series plot involves plotting the daily, monthly and yearly rainfall data and observing the trend. If they exhibit irregular, aperiodic or unpredictable behavior, then it could be described as random or chaotic. On the other hand if they exhibit a regular repeating pattern, then the system exhibits either a periodic and quasi periodic behavior [17].

2.4.2 Phase portrait

A phase portrait is a two-dimensional visualization of the phase-space. It displays the attractor and unveils its dynamics. Chaotic systems exhibit distinct shapes, periodic systems exhibit limit cycle (closed curves) while quasi periodic systems exhibit torus shape [13].

2.4.3 Poincaré maps

The Poincaré map is that it represents a slice through the attractor of the dynamical system and it is a stroboscopic view of the phase portrait of the dynamical system; hence it can also be referred to as a stroboscopic map [18]. Poincaré maps of periodic systems shows a single point, quasi-periodic systems shows a closed curve while chaotic systems show distinct points. A summary of the different dynamical systems and their characteristics is shown in Table 1 [13].

Table 1. Different Dynamic Systems and the Structure of their Power Spectrum, Phase Portraits and Poincaré Maps

Solution of Dynamical System	Fixed	Periodic	Quasi Periodic	Chaotic
Power spectrum	-	Single dominant peak	Dominant peak and other sub-peaks	Broad band noise with continuum of frequencies; may peak at $f_o = 0$
Phase portrait	Point	Closed Curve	Torus	Distinct Shapes
Poincaré Maps	-	Point	Closed Curve	Space filling or Ergodic points

2.4.4 Correlation dimension

The correlation dimension gives a measure of the complexity or number of active degrees of freedom excited by the system [19]. The Grassberger-Procaccia algorithm is used to compute the correlation dimension in this work using the correlation integral. For any set of M points in an *m*-dimensional phase space, the correlation integral or correlation sum (spatial correlation of points) $C(r)$ is computed by the equation [20]:

$$C_m(r) = \lim_{N\to\infty} \frac{2}{N(N-1)} \sum_{i=1}^{M} \sum_{j=i+1}^{M} H\left(r - \|\vec{x}_i - \vec{x}_j\|\right)$$

(10)

$H(x)$ is the Heaviside function and $\|\ldots\|$ is the Euclidean norm, while r is the scaling parameter. The correlation integral measures the fraction of the total number of pairs of phase points that are within a distance r from each other. For chaotic time series, the correlation integral power law for small values of r takes the form:

$$C(r) \sim r^{v} \qquad (11)$$

Thus, the correlation dimension v is given by:

$$v = \lim_{r\to 0} \lim_{M\to\infty} \frac{\log C(r)}{\log r}$$

(12)

Hence, a log-log graph of the correlation integral versus the scaling parameter, r will yield an estimate of the correlation dimension *v,* which is computed from the slope of a least-square fit of a straight line over a large length scale of r. For chaotic systems, the correlation exponent curve for a range of values of embedding dimension (say m = 2 to 30) usually saturates at values beyond its actual embedding dimension. The saturation value of the correlation exponent plot gives the correlation dimension and the value of the embedding dimension at which the saturation of the correlation exponent curve occurs generally provides an upper bound on the number of variables sufficient to model the dynamics [17]. The dynamics of different systems is described in Fig. 1 [3]:

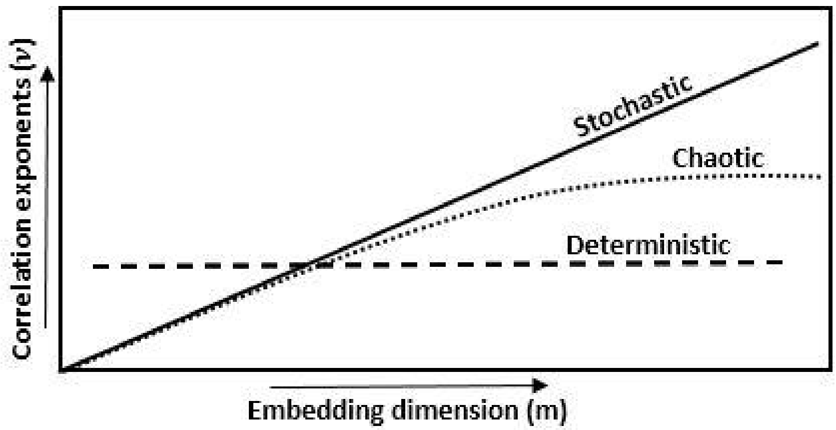

Fig. 1. Characterization of systems based on their correlation exponent plot

Furthermore, If the calculation of correlation dimension leads to a finite integer value, the underlying dynamics of the system is considered to be dominated by some strong periodic phenomena whereas if the value is fractional (and usually small) then the system is considered to be dominated by low dimensional deterministic chaotic dynamics governed by the geometrical and dynamical properties of the attractor [21].

2.4.5 Lyapunov Exponents

Lyapunov exponents (λ) are the average rates of exponential divergence or convergence of nearby orbits in phase space and is a fundamental property that characterizes the rate of separation of infinitesimally close trajectories [22]. It is mathematical given by:

$$\lambda_1(i) = \frac{1}{i.\Delta t} \cdot \frac{1}{M-i} \cdot \sum_{j=1}^{M-i} \ln \frac{d_j(i)}{d_j(0)} \tag{13}$$

Δt is the sampling period of the time series, M is the number of reconstructed phase points and $d_j(i)$ is the distance between the jth pair of nearest neighbors after i discrete-time steps, i.e., $i.\Delta t$ seconds. The nearest neighbor, X_j, is found by searching for the point that has the least distance to the particular reference point, X_j. This is expressed as:

$$d_j(0) = \min_{X_j} \lVert X_j - X_j \rVert \tag{14}$$

$d_j(0)$ is the initial distance from the jth point to its nearest neighbor $\hat{j}$. A positive Lyapunov exponent indicates chaotic behavior, a negative value indicates a dissipative system i.e. a stable fixed point while a zero Lyapunov exponent indicates conservative system i.e. a periodic one or stable limit cycle [23]. The method used in this work to compute the largest Lyapunov exponent was developed by Rosenstein *et al.* in 1992 [24].

2.4.6 Phase Space Reconstitution

In order to effectively carry out nonlinear analysis, phase space reconstruction has to be done so as to draw out a multi-dimensional description of system in an embedded space called state space. The method of delays was thus employed to achieve this [22],[25]. For a generalized time series $\{x_1, x_2, \ldots, x_N\}$, the attractor can be reconstructed in a m-dimensional phase space of delay coordinates in form of the vectors:

$$X_n = [x_n, x_{n+\tau}, x_{n+2\tau}, \ldots, x_{n+(m-1)\tau}] \tag{15}$$

τ is the time lag, and m is the embedding dimension. The time delay τ is evaluated in this work using the method of average mutual information (AMI) developed by Cellucci *et al*. in 2003 [26]. In order to obtain the time delay, the value of the lag length at the first local minimum of the AMI

plot corresponding to the delay time of the time series [3],[17]. The minimum embedding dimension, m was computed using the method of "False Nearest Neighbors (FNN)" which was developed by Kennel *et al.* in 1992 [27]. By plotting the percentage of FNN against increasing embedding dimension values, a monotonic decreasing curve is observed and the minimum embedding dimension can be evaluated from the point where the percentage of FNN drops to almost zero or a minimum value.
The mean period, P of the data was computed as the inverse of the peak period of the fast Fourier transform. The mean period or periodicity P in a time series removes cyclic/seasonal variations in a time series data by seasonal differencing technique. The phase space reconstruction will not be properly achieved and the deterministic components of the data will not be adequately revealed if the data is not made stationary and this could lead to misleading results in the nonlinear analysis of the data [28].

2.5 Study Area and Data Source

Katsina state, also known as the home of hospitality, is located in the North-Western region of Nigeria. The state is located within the coordinates 12°15' N , 7°30' E and 12°25' N , 7°50' E, and was created on 23rd September, 1987. It covers a total land area of 24,192 km^2 with a population density of 160 /km^2 and its landscape is largely dominated by the Sahel savannah vegetation. Katsina state experiences two dominant seasons: the rainy and dry season, with the Hausa-Fulani who are predominantly farmers being the largest ethnic group in the state [29]. The data used in this research was obtained from the Nigerian Meteorological Agency (NiMet) Abuja. It comprises of secondary data made up of daily average rainfall (mm) recorded in Katsina from 1st January, 1990 to 31st December 2015, a period of twenty-six years.

3. RESULTS AND DISCUSSION

The results of the behavioral analysis of rainfall pattern in Katsina is presented in this section.

3.1 Results of the Statistical Analysis

The statistics of daily rainfall (mm) is displayed in Tables 2:

Table 2. Statistics of daily rainfall in Katsina

Statistic	Value
No. of data	9490
No. of zeros	8241 (86.8%)
Mean (mm)	1.594
Standard Deviation (mm)	6.525
Variance (mm)	42.574
Coefficient of Variation (cv)	4.093
Signal-to-noise ratio	0.244
Maximum value (mm)	156.00
Minimum value (mm)	0.00
Kurtosis	78.2994
Skewness	6.8979

The results in Table 2 show a generally low overall mean value of daily rainfall (1.59 mm) and a high variability ($cv = 4.09$). Furthermore a kurtosis of 78.3 and Skewness of 6.9 (skew to the right) with a large amount of zeros (86%) in the data used indicates a sparse irregular distribution (high outlier-prone data) of rainfall in Katsina over the last 26 years. This is attributed to the fact that Katsina is located in the Sahel savannah region of Nigeria within the Sahara desert region, hence the limited and sparse amount of rainfall received in the town. Fig. 2. (a), (b), (c) and (d) shows time series plots of daily, monthly and yearly rainfall in Katsina.

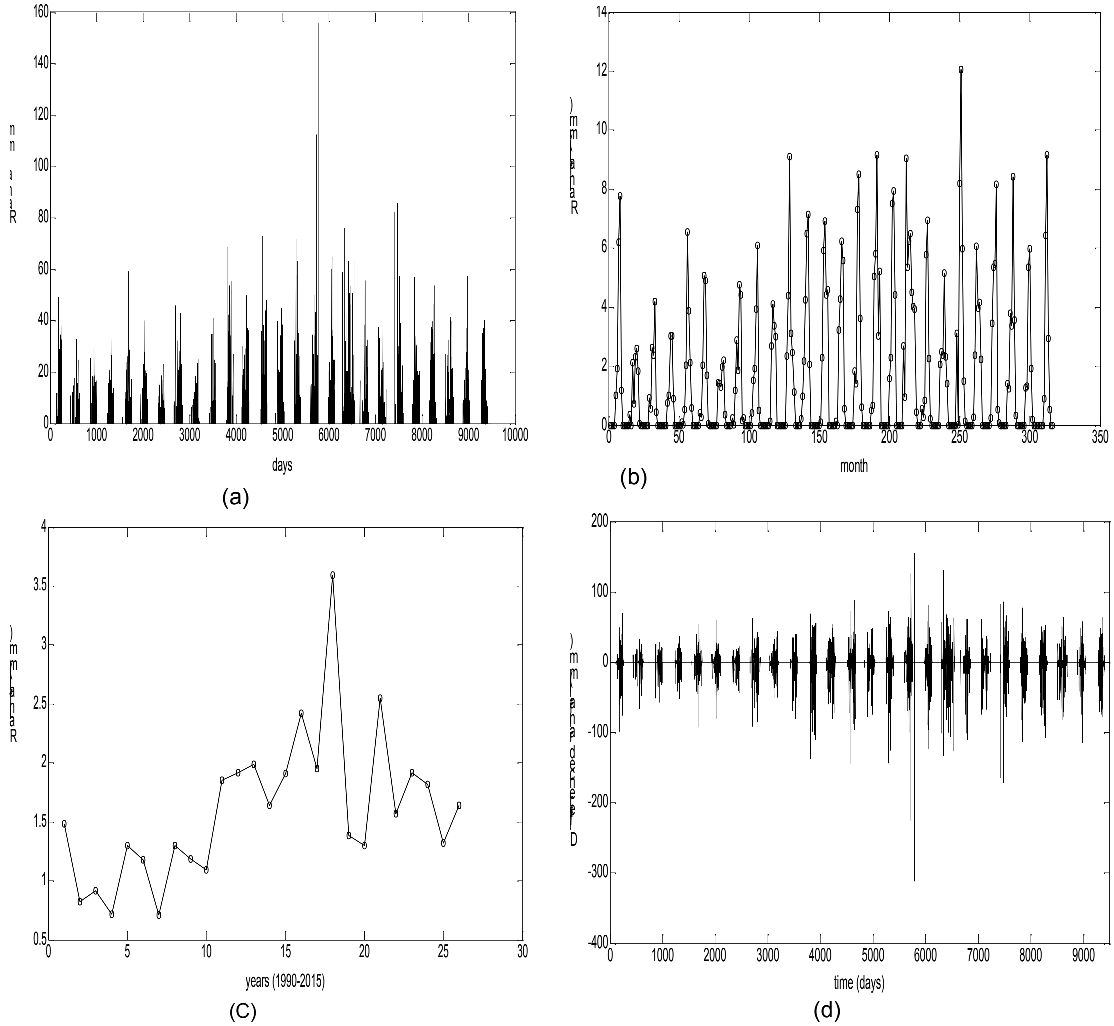

Fig. 2. Time Series for: (a) Daily, (b) Monthly, and (c) Yearly (d) Differenced rainfall time series for Katsina from 1990-2015

3.2 Trend Analysis

The summary of the trend analysis of the converted annual rainfall data using the Mann-Kendall trend test, Sen's slope estimator and Pearson's correlation coefficient are displayed in Table 3 and Fig. 3.

Table 3. Summary of the Mann-Kendall analysis for annual rainfall in Katsina

Variable	Annual Rainfall (mm)
Pearson's correlation coefficient (*R*)	0.5029
Kendall tau	0.3846
Mann-Kendell coefficient S	125
Z statistic	2.7332
Hypothesis test (h=1: significant, h=0: not significant)	h = 1
Trend description (from R and Z values)	Increasing trend

Trend Significance	Significant

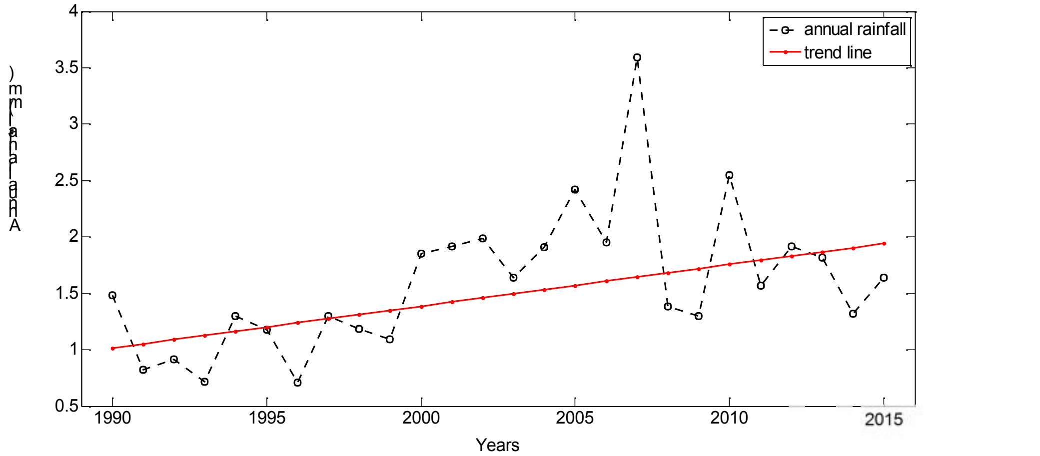

Fig. 3. Annual Rainfall trend for Katsina using Sen's Slope Model, $y = 0.037t - 72.64$ (increasing trend)

The trend analysis results in Table 3 (Mann-Kendall test) and Fig. 2 (Sen's slope estimator) indicates that the trends of the annual rainfall in Katsina is significant as the Z-statistic computed (2.73) is greater than the z-value at the level of significance (1.96). This implies an increasing trend in the mean annual rainfall in Katsina state. Hence there could be an increased risk of occurrences of flooding and surface run-off/erosion in the nearest future.

3.3 Results of Spectral Analysis

The result of the spectral analysis of daily rainfall in Katsina from 1990 to 2015 is displayed in Fig. 4.

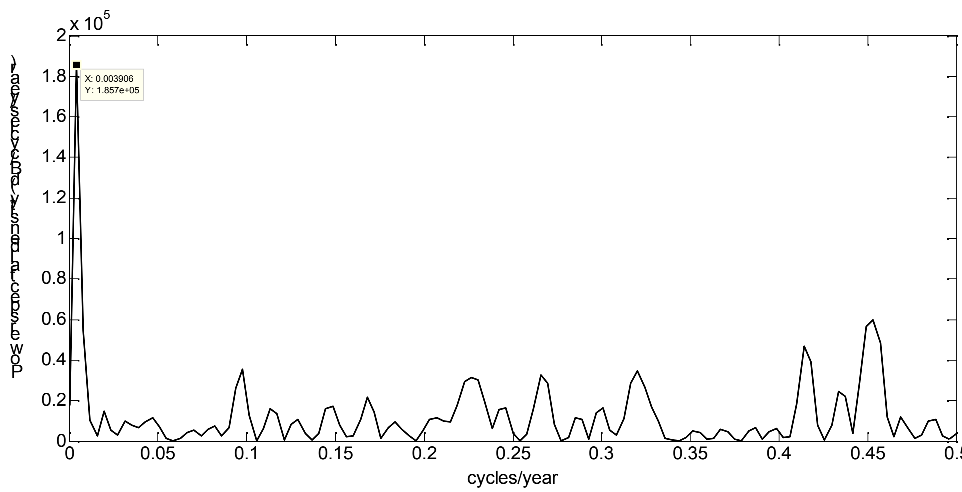

Fig. 4. Power Spectrum of Rainfall in Katsina showing the Dominant Frequency

The result of the spectral analysis displayed in Fig. 4 shows that the rainfall in Katsina has a single dominant peak and some smaller peaks indicating a quasi-periodic behavior with a mean annual cycle of 256 days rainfall over the last 26 years.

3.4 Results of the Nonlinear Analysis

Fig. 5 shows the estimation of time lag using the method of average mutual information (AMI). A delay time of 6 days was calculated for the rainfall dataset. Fig. 6 on the other hand illustrates the determination of the optimum embedding dimension using the method of false nearest neighbors (FNN). The rainfall data for Katsina was found to have an embedding dimension of eleven ($m = 5$). The embedding dimension value obtained ($m = 5$) indicates that the rainfall in Katsina requires a maximum of 5 independent variables (degrees of freedom) to model its dynamics.

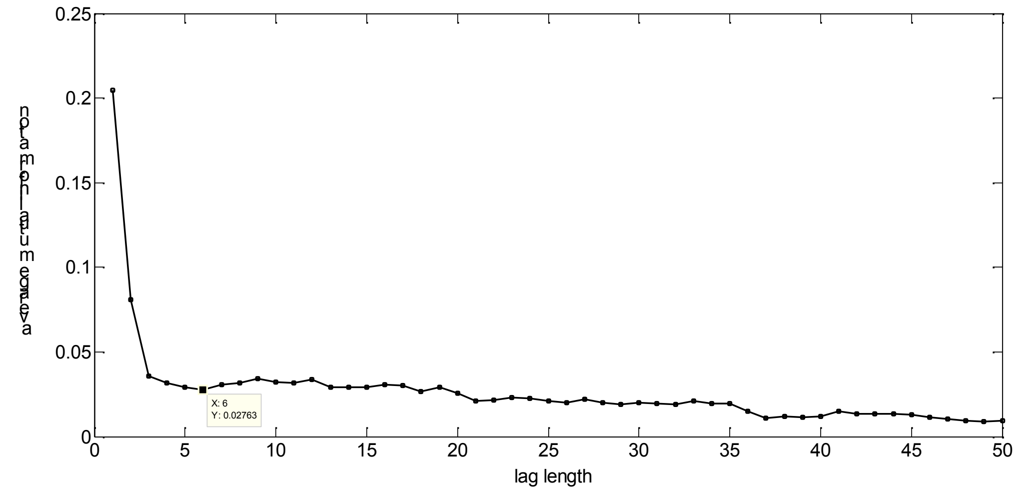

Fig. 5. Estimation of time lag using the method of AMI (τ = 6 days)

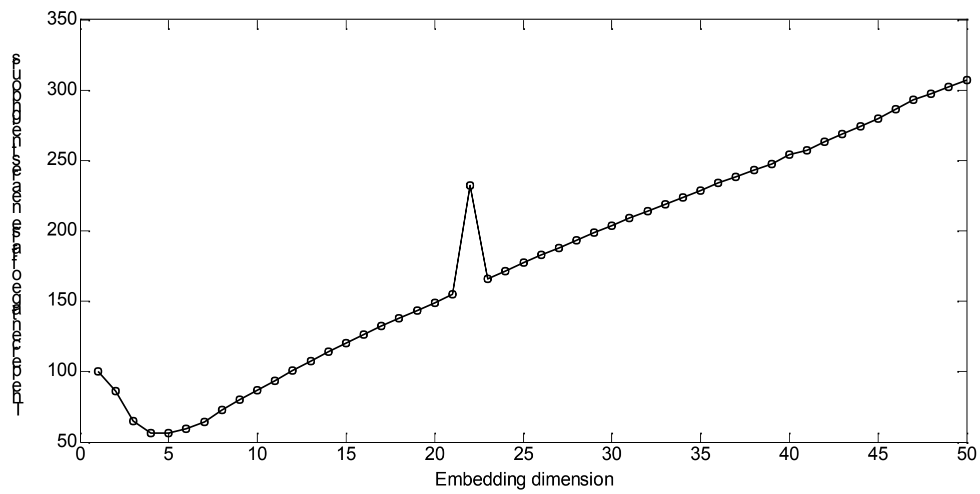

Fig. 6. Percentage of FNN for Rainfall in Katsina (m = 5)

Fig. 7 and 8 show the phase portrait and Poincaré map for rainfall constructed using the time lag and embedding dimensions calculated. The phase portrait exhibits a sponge-like geometry of distinct shapes tending towards the origin (zero) while the Poincaré map shows scattered distinct points also tending towards an equilibrium point (attractor) indicating the presence of a dissipative-damped random cycles in the dynamics of the rainfall time series. These plotted phase points are concentrated at the origin due to the numerous zeros (86.8%) in the rainfall dataset which is as a result of the sparse distribution of rainfall in Katsina.

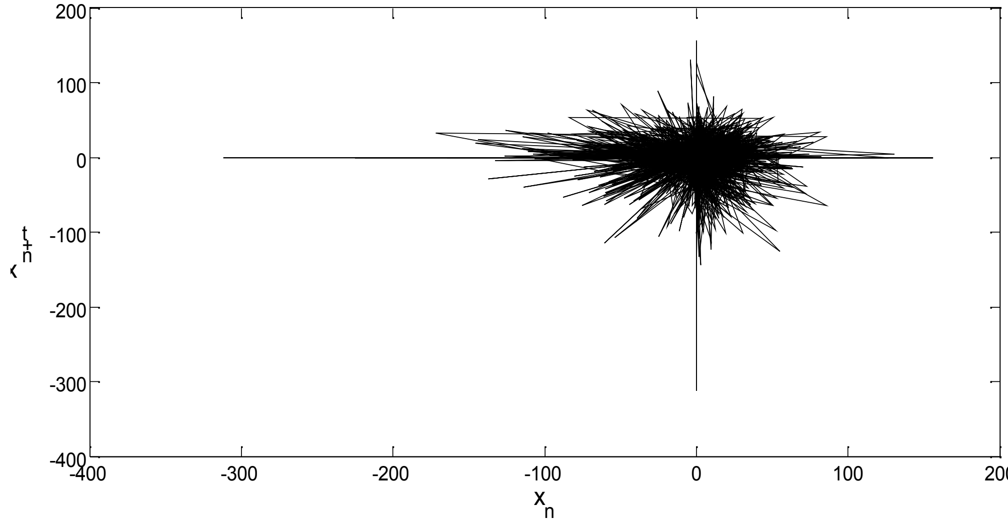

Fig. 7. Phase portrait of daily rainfall in Katsina

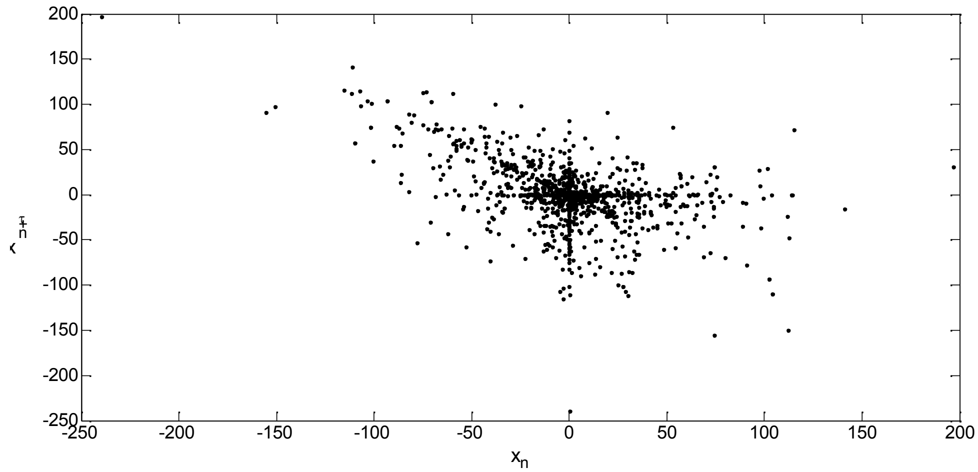

Fig. 8. Poincaré map of daily rainfall in Katsina

The correlation dimension was then calculated for the rainfall datasets using the time lag τ =6 and for increasing embedding dimensions, *m*, from 2 to 50. Fig. 9 is a plot showing the relationship between the correlation function *C(r)* and the radius *r* (i.e. $\log C(r)$ versus $\log r$) for increasing embedding dimension *m* while Fig. 10 shows the relationship between the correlation exponents and the embedding dimension values *m*. It is observed from Fig. 10 that the correlation exponent values keep increasing with increase in embedding dimension and thus failure of the plot to saturate indicates a likely stochastic behavior in the daily rainfall time series.

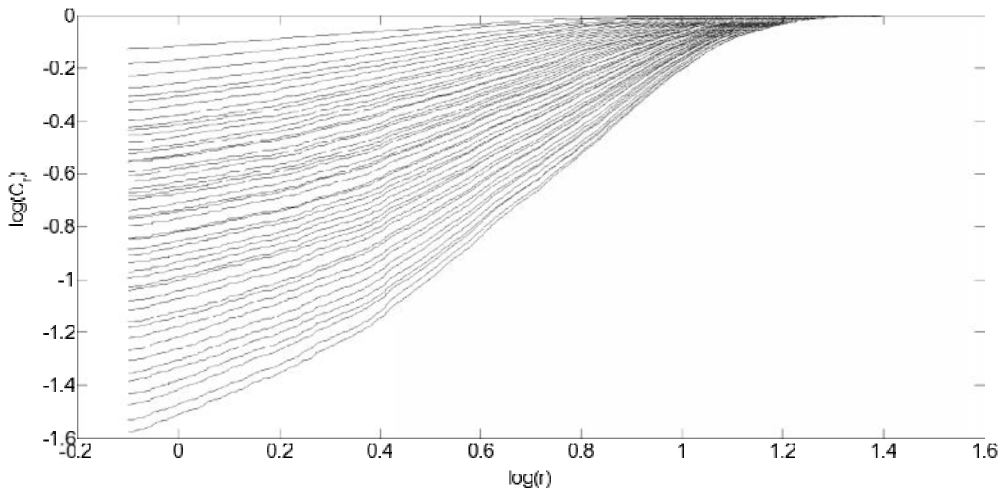

Fig. 9. (a) log-log plot showing the relationship between the Correlation Integral *C(r)* and the Scaling Radius *r* for different values of embedding dimension for daily rainfall in Katsina from 1990-2015

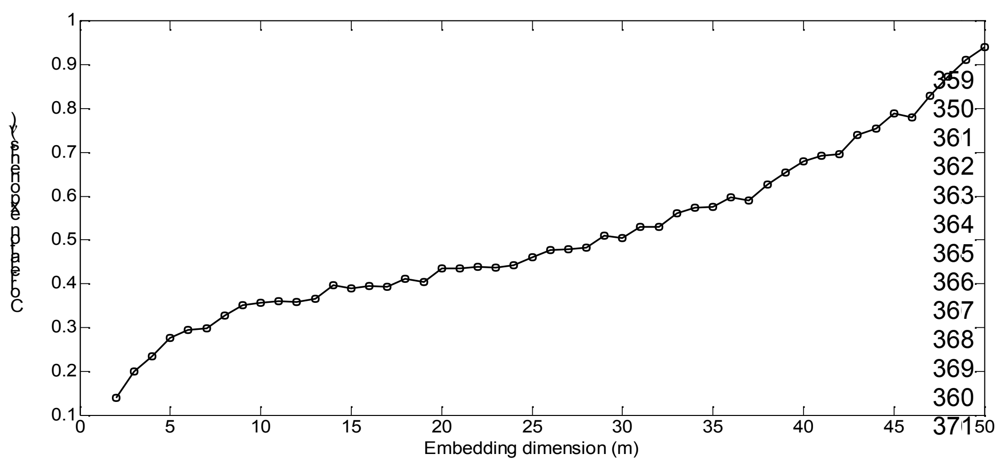

Fig. 10. Relationship between correlation exponent and embedding dimension *m* for daily rainfall in Katsina from 1990-2015

The Lyapunov spectrum obtained from the computation of the Lyapunov exponent for daily rainfall in Katsina using Rosenstein's algorithm is displayed in Fig. 11 while the details of the Lyapunov exponents for increasing values of embedding dimension is presented in Table 4.

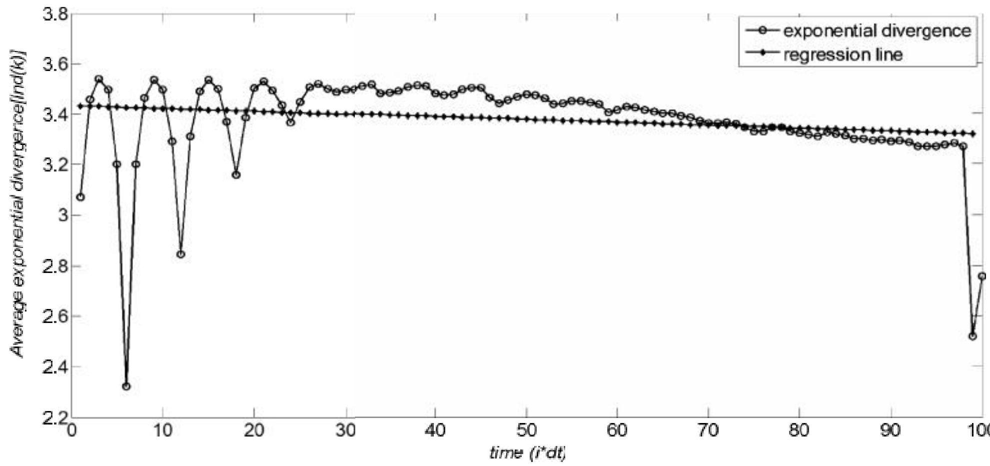

Fig. 11. The Lyapunov Spectrum for the Estimation of the Largest Lyapunov Exponent for Rainfall in Katsina from 1990-2015.

Table 4. The Lyapunov exponent values from m=1 to 5

Embedding dimension (m)	Lyapunov exponent (λ)
1	-0.001964050055998
2	-0.002785724113455
3	-0.002077999517956
4	-0.001332489877303
5	-0.001157108333026

*Largest Lyapunov exponent, λ = -0.001157/day

The largest Lyapunov exponent for the rainfall time series in Katsina was computed and found to be -0.001157/day. The negative near zero values of the Lyapunov exponent indicate that the daily rainfall in Katsina over the last 26 years exhibits a stable fixed point (dissipative) behavior which is likened to a critically damped oscillator as the values tend towards an equilibrium point (zero) at certain irregular intervals. This also indicates that the daily rainfall in Katsina is sparse and stochastic but has relatively fair predictability.

4. CONCLUSION

In this paper, a behavioral analysis of rainfall pattern in Katsina from the year 1990-2015 was carried out. The outcome of this analysis indicates that the rainfall in Katsina exhibits an increasing trend with high variance and stochastic behavior. A maximum of five (5) independent variables is required to model the daily rainfall in Katsina while the rainfall is sparse and has good predictability in the next couple of days. It is recommended that adequate measures such as irrigation and flood control measures like building of more drainages and dams to curb the menace of irregular rainfall, flash floods and other effects of global warming and climate change which are eminent in the northern part of Nigeria.

REFERENCES

1. Fathima T, Jothiprakash V. Behavioural Analysis of a Time Series-A Chaotic Approach, Sâadhanâ, 2014; 39(3): 659-676.

2. Lorenz E. Deterministic non-periodic flow. Journal of the Atmospheric Sciences. 1963; 20(2): 41.

3. Jani R, Ghorbani MA, Shamsai A. Dynamics of Rainfall in Ramsar, Journal of Applied Science and Agriculture. 2014; 9(4): 1371-1378.

4. Lai L. Intelligent weather forecast. Third international conference on machine learning and cybernetics. Shanghai; 2004.

5. Sharma A, Manoria M. A Weather Forecasting System using concept of Soft Computing: a new approach. AIP conference proceedings India. 2007; 923: 275.

6. MathWorks Inc. Skewness and Kurtosis. MATLAB Statistics Toolbox. R2014a.

7. Correlation Coefficient and Coefficient of Determination. Statistics-2. 2015. Accessed on 13 September 2014. Available: http://mathbits.com/MathBits/TISection/Statistics2/Correlation .html. Accessed on 13/8/2014.

8. McBean E, Motiee H. Assessment of Impact of Climate Change on Water Resources: A Long Term Analysis of the Great Lakes of North America. Hydrology and Earth System Sciences. 2008; 12**:** 239–255.

9. Christoph A, Frei S. Analysis of Climate and Weather Data: Trend Analysis. Accessed 10 October 2015. Available: http://www.iac.ethz.ch/edu/courses/master/electives/acwd/trend. pdf.

10. Olofintoye O, Sule BF. Impact of Global Warming on the Rainfall and Temperature in the Niger Delta of Nigeria. USEP: Journal of Research Information in Civil Engineering. 2010; 7**(**2): 33-48.

11. Khambhammettu P. Mann-Kendall Analysis, Annual Groundwater Monitoring. Report of HydroGeologic Inc. California: Fort Ord; 2005.

12. Salmi T, Määttä A, Anttila P, Ruoho-Airola T, Amnell T. Detecting Trends of Annual Values of Atmospheric Pollutants by the Mann-Kendall Test and Sen's Slope Estimates –The Excel Template Application Makesens. Finnish Meteorological Institute Publications on Air Quality Helsinki, Finland. 2002; 31.

13. Ozer B, Akin, E. Tools for Detecting Chaos. Sau Fen Bilimleri EnstitusuDergisi. 2005; 9(1): 60-66.

14. Shannon H. Power Spectrum in MATLAB. BitWeenie: digital signal processing. 2013. Accessed on 4 September 2013. Available: http://www.BitWeenie.html.

15. Burrus C, Parks T. DFT/FFT and Convolution Algorithms. New York, John Wiley and Sons; 1985.

16. Telgarsky R. Dominant Frequency Extraction. arXiv: 1306.0103. 2013; 1: 1-12.

17. Echi MI, Tikyaa EV, Isikwue BC. Dynamics of Rainfall and Temperature in Makurdi, International Journal of Science and Research, 2015; 4(7): 493-499.

18. Velickov S. Nonlinear Dynamics and Chaos with Applications to Hydrodynamics and Hydrological Modeling. London: Taylor and Francis Group plc; 2006: 76-79.

19. Rothman D. Nonlinear dynamics I: Chaos-Lyapunov exponents. MIT open courseware on Dynamics and Relativity. 2012. Accessed on 9 September 2013. Available: http://archive.org /details/flooved1828.

20. Grassberger P, Procaccia I. Characterisation of Strange Attractors. Physics Review letters. 1983; 50: 346-349.

21. Lugt PM. Grease Lubrication in Rolling Bearings. USA: John Wiley and sons; 2012: 252-253.

22. Takens F. Detecting Strange Attractors in Turbulence. Lecture Notes in Mathematics. 1980; 898: 366.

23. BenSaïda A. Are Financial Markets Stochastic? A Test for Noisy Chaos. American International Journal of Contemporary Research. 2012; 2(8): 57.

24. Rosenstein M, Collins J, De Luca C. A practical method for calculating largest Lyapunov exponents from small data sets. Physica D. 1993; 65: 117-134.

25. Packard N, Crutchfield J, Farmer J, Shaw R. Geometry from a Time Series. Physics Review Letters. 1980; 45: 712.

26. Cellucci C, Albano, A, Rapp, P. Comparative Study of Embedding Methods. Physical Review E. 2003; 67(6): 1-13.

27. Kennel M. Brown R. Abarbanel H. Determining embedding dimension for phase-space reconstruction using a geometrical construction. Physical Review A. 1992; 45(6): 3403-3411.

28. Fuwape IA, Ogunjo ST, Oluyamo SS. Rabiu AB. Spatial variation of deterministic chaos in mean daily temperature and rainfall over Nigeria. Theor Appl Climatol., Springer-Verlag Wien. 2016; DOI 10.1007/s00704-016-1867-x.

29. Wikipedia. Katsina state. Accessed on 18 February 2017. Available: http://en.wikipedia.org/wiki/katsina_state. Accessed on 18/02/2017.